

New Cd(II), Mn(II) and Ag(I) Schiff Base Complexes : Synthesis, Characterization, DNA Binding and Antimicrobial Activity

Laila H. Abdel-Rahman¹, Ahmed M. Abu-Dief^{1,*}, Rafat M. El-Khatib¹, Shima Mahdy Abdel-Fatah¹ and Amin Abdou Seleem²

¹Chemistry Department, Faculty of Science, Sohag University, 82534Sohag, Egypt.

²Zoology Department, Faculty of Science, Sohag University, 82534 Sohag, Egypt.

Received: 14 May 2016, Revised: 16 Jun. 2016, Accepted: 18 Jun. 2016.

Published online: 1 Sep. 2016.

Abstract: Some Cd (II), Mn (II) and Ag (I) complexes derived from Schiff base ligand, obtained by the condensation of 4-Nitrobenzaldehyde and 2-amino-3-hydroxypyridine were synthesized. The complexes were characterized by elemental analysis, molar conductivity, magnetic susceptibility, IR, UV-Vis spectral data and thermal analysis. The complexes were found to be non-electrolytic in nature depending on value of molar conductance. From the spectral data, an octahedral geometry has been approached for all the complexes except Ag (I) complex which is tetrahedral. Moreover, the metal complexes have been tested for their antibacterial and antifungal activity. Furthermore, DNA interaction of these complexes was tempted by using Electronic spectra, viscosity measurements and gel electrophoresis. The experimental results indicated that the investigated complexes could associate with DNA via intercalative mode and showed a different DNA binding activity.

Keywords: Synthesis, molar conductance, antifungal activity, antibacterial activity, DNA interaction.

1 Introduction

Schiff bases are condensation outputs of primary amines and carbonyl compounds and they were discovered by a German chemist, Nobel Prize winner, Hugo Schiff in 1864. Schiff bases are characterized by an imine group $-N=CH-$, which helps to elucidate the mechanism of transamination and racemization interaction in biological system [1]. It exhibits antibacterial and antifungal effect in their biological properties [1-3]. Metal-imine complexes have been widely investigated due to antitumor and herbicidal utilization. They can work as models for biologically important species. The chelating ability and biological implementations of metal complexes have attracted remarkable attention [1,4]. Metal complexes having N, O donor atoms are very remarkable because of their significant biological properties such as antibacterial [5], antifungal, anticancer, and herbicidal activity. Nitro aromatic compounds are relatively rare in nature and have been introduced into the environment mainly by human activities. This serious class of industrial chemicals is widely used in the synthesis of many assorted products, including dyes, polymers, pesticides, and explosives[6]. Two thiocyanato bridged dinuclear copper (II) complexes originated from 2,4-dibromo-6-[(2-diethylaminoethylimino)methyl] phenol and 4-nitro-2-[(2-

ethylaminoethylimino) methyl]phenol showed wide range of antibacterial activity[7]. The present aim of the work is to synthesize a Schiff base derived from 2-amino-3-hydroxypyridine and 4-nitrobenzaldehyde and to prepare its transition metal complexes, characterize them and make survey their antibacterial and anti-fungal potencies. We also study their interaction with DNA.

2 Experimental

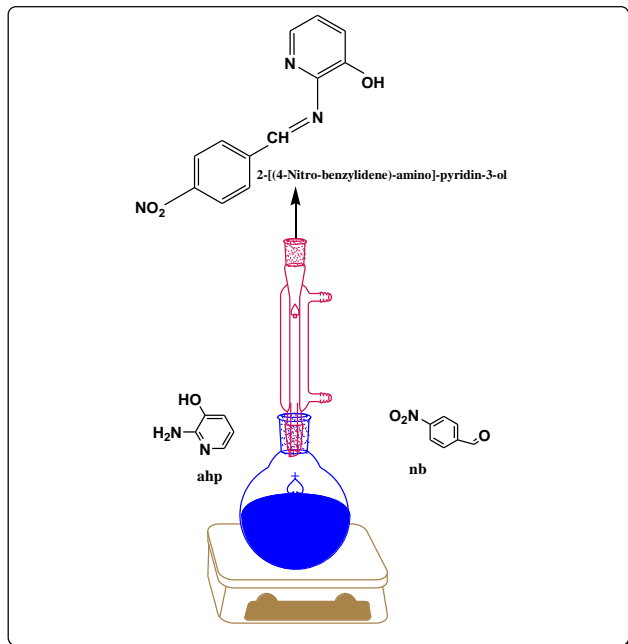
All the starting materials of chemicals utilized in this investigation Such as 4-nitrobenzaldehyde (nb), 2-amino-3-hydroxypyridine, the metal salt ($MnCl_2 \cdot 4H_2O$, $AgNO_3 \cdot 6H_2O$, $CdNO_3 \cdot 4H_2O$), Calf thymus DNA (CT-DNA) and Tris[hydroxymethyl]-aminomethane (Tris) were obtained from Sigma–Aldrich Chemie (Germany). Spectroscopic grade ethanol and HCl products were used.

2.1. Synthesis of Schiff base ligand

An equimolar mixture of 2-amino-3-hydroxypyridine (1mmol, 0.11 g) and 4-nitrobenzaldehyde (1 mmol, 0.15 g) dissolved in ethyl alcohol and mixture was refluxed for 2 hours. The reaction mixture was filtered, rinsed with water

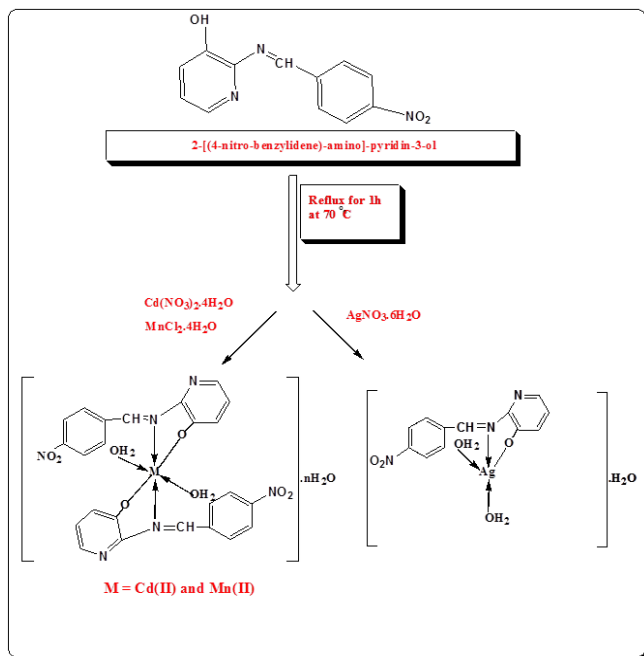
* Corresponding author E-mail: ahmed_benzoic@yahoo.com

and recrystallized from ethyl alcohol. The Schiff base was dried under reduced pressure in a desiccator. The purity of synthesized compounds was checked by TLC utilizing silica gel G (yield: 81 %) as shown in (scheme.1).



Scheme (1): synthesis of Schiff base ligand (ahpnb), where ahp = 2-amino-3-hydroxypyridine and nb = 4-nitrobenzaldehyde.

2.2. Synthesis of metal complexes



Scheme (2): The suggested structures of ahpnbCd, ahpnbMn, ahpnbAg complexes, ahpnbCd: n =4 and ahpnbMn: n= 8.

The ligand (2 mmol,) and the metal salt (1 mmol) in 50 ml ethanol was refluxed for 1 hour. In all the cases the ligand concentration was slight excess of 1:2 (metal: ligand molar ratio)[8]. After refluxing the solid mass separated filtered through and the residue was washed several times with hot methanol until the washing were free of the increase of ligand these complexes finally dried under vacuum desiccators over fused calcium chloride, (yield: 65-76%) as shown in (scheme.2).

2.3. Physical measurements

Melting point for Schiff base ligand and decomposition points for complexes were carried out on a melting point apparatus, Gallenkamp, UK. The IR spectra of the Schiff base and its metal complexes were recorded on a FTIR Shimadzu model 8101 spectrophotometer in the 4000-400 cm^{-1} region in KBr powder. C, H and N were estimated by using elemental analyzer Perkin-Elmer model 240c. The electronic spectra of the complexes were recorded in HPLC grade DMF and DMSO using 10 mm matched quartz cells on PG spectrophotometer model T+80 in the region of 800-200 nm. Molar conductivity mensuration were recorded on JENWAY conductivity meter model 4320 at 298 K using ethanol as solvent. Magnetic measurements of the complexes were performed on Gouy's balance at room temperature. Thermal decomposition studies were registered in a static nitrogen with a heating rate of 10°C/min, using Shimabzu Corporation 60H instrument. ^1H NMR spectra were recorded in DMSO on BRUKER model 400 MHz spectrophotometer using TMS as an internal standard (δ ppm) and DMSO-*d*6 as the solvent. The values of absorbance of 5×10^{-3} M of each complex were measured at different PH values. The pH values were adjusted by using a series of Britton universal buffers [9]. pH measurements were carried out using HANNA 211 pH meter at 298 K.

2.4. Antimicrobial activity

The *in vitro* biological screening effects of the investigated compounds were tested against the gram negative(bacteria *Escherichia coli*, *Serratia marcescense*) and gram positive bacteria *Microoccus luteus* by the well diffusion procedure (agar cup method) using agar nutrient as the medium. While antifungal activity was carried out using glucose yeast extract media (GYE) against *Aspergillus flavus* , *Getrichm candidum* and *Fusarium oxysporum*. The stock solutions were prepared by dissolving the compounds in DMSO. In a typical procedure, a well was made with the help of borer on the nutrient medium plate which was formerly inoculated with microorganisms. The well was filled with the different concentration of test solution utilizing a micropipette and incubated at 37°C for 24 hrs (bacteria) and 48 hrs (fungi). **Ofloxacin** and **Fluconazol** were used as control against the bacteria and fungi respectively. During incubation period, the test solution

deployed and the growth of the inoculated microorganisms was affected. Antibacterial activity was indicated by the presence of patent zone of inhibition around the wells. The zone of inhibition was measured in mm [2,3,10].

2.5. DNA binding experiments.

All the experiments comprising the interaction of the complexes with DNA were carried out in Tris-HCl buffer (50 mM, pH 7.2). CT-DNA was decontaminated by centrifugal dialysis before use. A solution of calf thymus DNA in the buffer offered a ratio of UV absorbance at 260 and 280 nm of about >1.86, indicating that the DNA was sufficiently free from protein contamination [2,3,11, 12]. The concentration of DNA was determined by monitoring the UV absorbance at 260 nm using $\epsilon_{260} = 6600 \text{ mol}^{-1}\text{cm}^2$. The stock solution was stored at 4°C and used within only one day [2,3,11,12].

2.5.1. Absorption spectral studies.

Absorption spectral titrations were implemented in (50 mM Tris-HCl buffer, pH 7.2) buffer at room temperature to investigate the binding tendency between CT - DNA and complex. The concentration of CT - DNA was determined from the absorption intensity at 260 nm with a ϵ amount of $6600 \text{ mol}^{-1}\text{cm}^2$. Absorption titration experiments were performed by varying the concentration of the CT - DNA (0 - 40 μM) keeping the complex concentration (10 μM) as constant. The absorbance (A) was recorded after each accession of CT - DNA. The stock solution was stored at 4°C and used within only one day. In order to eliminate the absorbance of the CT-DNA an equal amount of the same was added to both the compound solution and the reference solution. The intrinsic binding constant, K_b for the complexes was determined from the spectral titration data utilizing the following equation :

$$\frac{[DNA]}{(\epsilon_a - \epsilon_f)} = \frac{[DNA]}{(\epsilon_b - \epsilon_f)} + \frac{1}{K_b(\epsilon_b - \epsilon_f)} \quad (1)$$

Here, ϵ_a , ϵ_f , and ϵ_b are apparent, free and fully bound complex extinction coefficients respectively, Where, [DNA] is the concentration of DNA in base pairs. In particular, ϵ_f was determined from the calibration curve of the isolated metal complex; following the Beer's law. ϵ_a was foredoomed as the ratio between the tried on

absorbance and the metal(II) complex concentration, $A_{\text{obs}}/[\text{complex}]$. The data were fitted to the above equation with a slope equal to $1/(\epsilon_b - \epsilon_f)$ and y-intercept equal to $1/[K_b(\epsilon_b - \epsilon_f)]$ and K_b was obtained from the ratio of the slope to the intercept [2,3, 11, 12, 13]. The standard Gibb's free energy for DNA binding was calculated from the following relation [2, 3, 11, 12, 14]:

$$\Delta G_b^\circ = -RT \ln K_b \quad (2)$$

2.5.2. Viscosity experiments for interaction of the prepared complexes with DNA

Viscosity measures were made using an Oswald microviscometer, kept at constant temperature at 25°C in thermostat. The flow times were recorded for various concentrations of the complex (10–250 μM), keeping the concentration of DNA constant (250 μM). blending of the solution was made by bubbling the nitrogen gas through the viscometer. The average value of the three measures was used to evaluate the viscosity of the samples. The buffer flow time in seconds was recorded as t° . The prorated viscosities for DNA in the presence (η) and absence (η°) of the complex were calculated using the relation $\eta = (t - t^\circ)/t^\circ$. Where, t is the notified flow time in seconds and the values of the relative viscosity (η/η°) were plotted against $1/R$ ($R = [\text{DNA}]/[\text{Complex}]$) [2, 3, 11, 12, 15].

2.5.3. Agarose gel electrophoresis

The DNA cleavage experiment was conducted utilizing CT DNA by gel electrophoresis with the corresponding metal. The reaction mixture was incubated before electrophoresis experiment at 35°C for 30 min as follows: CT DNA 20 μM , 50 μM each complex. The samples sample (mixed with bromophenol blue dye at a 1:1 ratio) were electrophoresed for 45 min at 50 V on 1% agarose gel utilizing TBE buffer, pH = 8.3. After electrophoresis, the gel was stained utilizing 1 $\mu\text{g}/\text{cm}^3$ ethidium bromide (EB) and photographed under UV light using Lumix Digital camera [2, 3, 11, 12, 16].

3 Results and discussion

3.1. physicochemical properties

Table 1: The analytical and physical data of ligand and its metal complexes.

Compound	Colour	(m.p) and Decom. point	M.wt	Elemental Analysis calculated (found)			Cond. Λ_m ($\Omega^{-1}\text{cm}^2 \text{mol}^{-1}$)	μ_{eff} B.M.
				C	H	N		
ahpnb	Brown	245	243	40.88 (40.79)	2.83 (2.79)	11.92 (11.91)	6.80	-
ahpnbCd	Brick red	>300	704.4	40.06 (39.95)	3.89 (3.78)	11.68 (11.59)	3.5	diamagnetic
ahpnbMn	Dark green	295	718.9	35.66 (35.74)	3.46 (3.39)	10.40 (10.55)	8.11	5.68
ahpnbAg	Orange	>300	403.8	40.88 (40.79)	2.83 (2.79)	11.92 (11.91)	15.43	diamagnetic

All the compounds are tinted, solid, stable at room temperature. The Analytical and physical data of ligand and their metal complexes are recorded in (Table 1). The metal complexes exhibit 1:2 (metal-ligand) stoichiometry.

3.2. $^1\text{H-NMR}$ spectra

The $^1\text{H-NMR}$ spectra of the L_1H ligand shows the signal at 7.25-8.46 (m) δ for aromatic proton and 9.39 (s) δ for azomethine proton. The peak at 6.41 (s) δ attributed to ($-\text{OH}$) group present in pyridine moiety, disappeared upon adding of D_2O [18,19].

3.3. Infrared spectra

The IR spectra of the complexes were compared with those of the free ligands in order to determine the embracing of the coordination sites in the chelation. Characteristic peaks in the spectra of the ligand and complexes were considered and compared. IR spectrum of the *ahpnb* ligand exhibited the most characteristic bands at 1621 cm^{-1} ($\nu(\text{C}=\text{N}$, azomethine) and 1288 cm^{-1} ($\nu(\text{C}-\text{O})$) [2,3, 19]. The formation of the Schiff base was noted from the absence of $\text{C}=\text{O}$ and NH_2 peaks in the ligand. The band at 1621 cm^{-1} due to the azomethine group of the Schiff base was shifted to lower frequencies ($1597\text{--}1603\text{ cm}^{-1}$) after complexation, indicating the bonding of nitrogen of the azomethine group to the metal ions. The phenolic $\text{C}-\text{O}$ stretching vibration that appeared at 1288 cm^{-1} in Schiff base shifted towards lower frequencies in the complexes. This approaches deprotonation of the phenolic OH group after its chelation with the metal ion. The appearance of broad bands at around $3480\text{--}3510\text{ cm}^{-1}$ in the spectra of complexes may be due to water molecules [20-23]. A band of medium intensity at $847\text{--}848\text{ cm}^{-1}$ (OH rocking) suggests the presence of coordinated water in all three complexes. In the low frequency region, the band of feeble intensity observed for the complexes in the region $734\text{--}739\text{ cm}^{-1}$ is attributed to $\text{M}-\text{O}$ and in the region $675\text{--}691\text{ cm}^{-1}$ to $\text{M}-\text{N}$ as shown in (Table 2).

3.4. Electronic spectra

The nature of the ligand field around the metal ion was inferred from the electronic spectra. The electronic absorption spectra of ligands and their complexes were registered at the wavelength range $800\text{--}200\text{ nm}$ and at 298 K . The ligand exhibits absorption bands in UV-Vis region around 344 nm which is assigned to $n\rightarrow\pi^*$ transition originating from the azomethene function of the Schiff base ligand [24]. The spectra of the complexes are dominated by charge transfer bands centered at $\lambda_{\text{max}} = 256\text{--}439\text{ nm}$ [25]. Furthermore, the charge transfer band is followed by a long and a broad band lying at 442 nm . This band could be mainly attributed to the $d \rightarrow d$ transition in *ahpnbMn* complex [2, 3, 26], except *Ag(I)* and *Cd(II)* complexes which there is no $d-d$ transition.

3.5. Magnetic moment measurements

The paramagnetic compounds will be attracted while the diamagnetic compounds repelled in a magnetic field. Therefore, paramagnetic substances will have positive susceptibilities. Thus, the magnetic susceptibility measures determine geometry of the complexes. Magnetic susceptibility measurements showed that the *ahpnbMn* complex has paramagnetic character and has octahedral geometry [11, 12, 27], except *Cd(II)* and *Ag(I)* complexes which is diamagnetic.

3.6. Thermal Analysis

The thermal behavior of the metal complexes showed that the hydrated complexes first lost molecules of water, followed by decomposition of the ligand molecules in the subsequent steps. The thermal analysis evaluation of the thermal stability of the metal complexes aided in the characterization of the metal complexes as shown in (Table 3). The final product is metal [2, 28].

3.7. Spectrophotometric Determination of the stoichiometry of the prepared complexes

Stoichiometry of complexes is investigated using the two methods, continuous-variations method (CVM), mole-ratio method (MRM). The methods used and the experimental results showed, the stoichiometry of the prepared complexes is 1:2. The curves of the continuous variation method (Figure.1) displayed maximum absorbance at mole fraction $X_{\text{ligand}} = 0.65\text{--}0.7$ illustrating the formation of complexes with metal ion to ligand ratio 1:2. Moreover, the data resulted from applying the molar ratio method support these results (Figure.2) [2, 3, 11, 12, 15, 29].

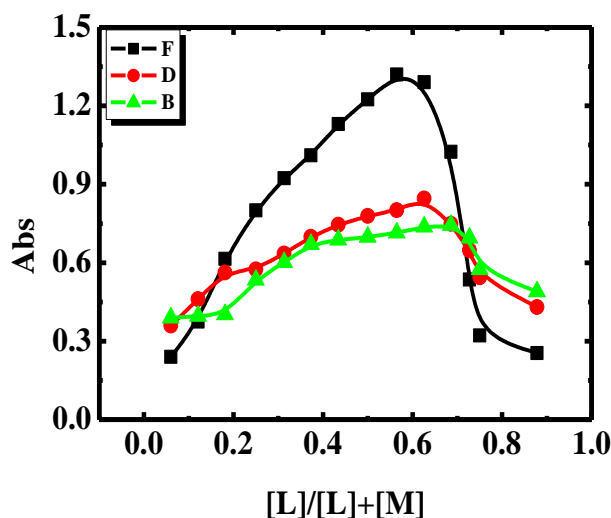


Figure. 1: Continuous variation plots for the prepared complexes in aqueous-alcoholic mixtures at $[\text{complex}] = 1 \times 10^{-3}\text{ M}$ and 298 K .

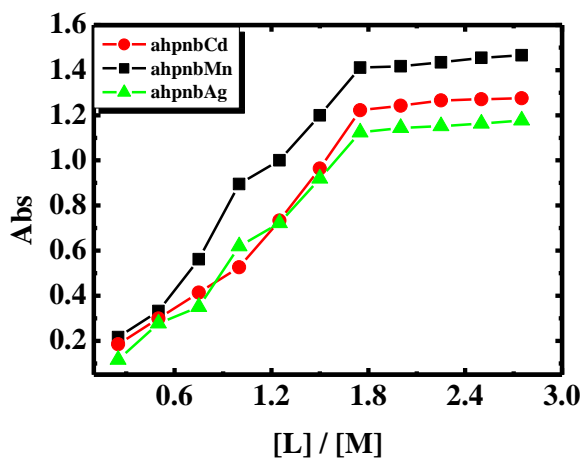
Table 2: Infrared spectral bands of Schiff base ligand and its complexes.

Compound	ν (OH/ H ₂ O)	(CH _{aro}) ν	(C=N) ν	ν (C-O) phenolic	(H ₂ O) ν Coordinat	(M-O) ν	(M-N) ν
ahpnb	3475(w)	3100(w)	1621(s)	1288(m)	-	-	-
ahpnbCd	3510(w)	3042(w)	1597(s)	1241(m)	848(s)	739(m)	691(m)
ahpnbMn	3480(w)	3090(w)	1603(s)	1285(m)	848(m)	736(s)	675(m)
ahpnbAg	3482 (w)	3041(w)	1603(s)	1284(m)	847(s)	734(s)	675(s)

s=Strong, m= medium, w= weak.

Table 3: Thermal Analysis data for metal complexes.

Complex	Degradation temperature °C	Lost fragment	Weight Loss%	
			theoretical	found
ahpnbCd	34-116	4H ₂ O	10.22	10.25
	116-438	2H ₂ O + C ₂₃ H ₁₅ N ₅ O ₅	67.71	67.68
	438-750	CHNO	6.10	6.08
	>750	Cd	15.98	15.99
ahpnbMn	34-190	8H ₂ O	20.03	20.00
	190-260	2H ₂ O + C ₁₂ H ₈ N ₄ O ₅	45.06	45.04
	260-498	C ₁₂ H ₈ N ₂ O	27.26	28.76
	>498	Mn	7.65	6.20
ahpnbAg	33-166	H ₂ O	4.45	4.50
	166-350	2H ₂ O + C ₆ H ₄ NO ₂	39.12	39.06
	350-465	C ₆ H ₄ N ₂ O	29.71	29.55
	>465	Ag	26.72	26.89

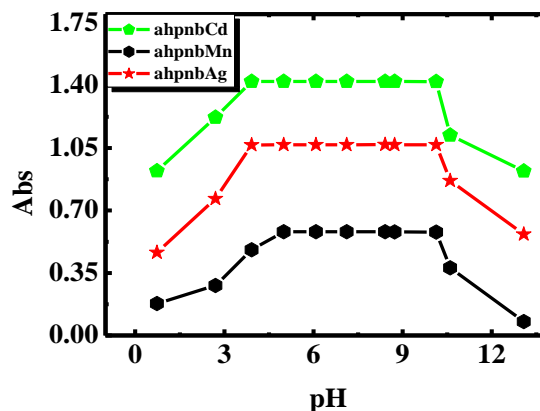
**Figure. 2:** Molar ratio plots for the studied complexes in aqueous- alcoholic mixtures [M]=[L]=1×10⁻³ and 298 K.

3.8. Determination of the apparent formation constants of the synthesized complexes.

The form constants (K_f) of the studied Schiff base complexes formed in solution were obtained from the spectrophotometric measures by applying the continuous variation method [29, 30, 31] (Table 4) according to the following equation:

$$K_f = \frac{A/A_m}{4C^2(1 - A/A_m)^3} \quad (3)$$

Where, A_m is the absorbance at the maximum formation of the complex, A is the arbitrary chosen absorbance values on either side of the absorbance mountain col (pass) and C is the initial concentration of the metal. As mentioned in, the obtained K_f values indicate the high stability of the studied complexes. The values of K_f for the investigated complexes increase in the following order: ahpnbAg > ahpnbCd > ahpnbMn.

**Figure. 3:** Dissociation curves of the prepared complexes in aqueous alcohol mixture at [complex] = 1 × 10⁻³ M and 298 K.

Moreover, the values of the constancy constant (pK) and Gibbs free energy (ΔG^\ddagger) of the prepared complexes are evaluated. The negative values of Gibbs free energy confirm that the reaction is spontaneous and favorable. The

Table 4: The formation constant (K_f), stability constant (pK) and Gibbs free energy (ΔG^\ddagger) values of the synthesized complexes in aqueous-ethanol at 298 K.

Complex	Type of complex	K_f	pK	ΔG^\ddagger kJ mol ⁻¹
[Cd(ahpnb) ₂ (H ₂ O) ₂].4H ₂ O	1:2	1.12×10^{11}	11.04	-63.00
[Mn(ahpnb) ₂ (H ₂ O) ₂].8H ₂ O	1:2	6.14×10^{10}	10.78	-61.51
[Ag(ahpnb)(H ₂ O) ₂].H ₂ O	1:1	3.41×10^{11}	11.53	-65.76

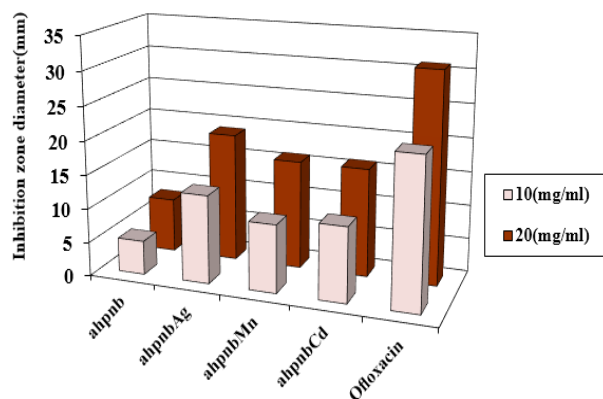
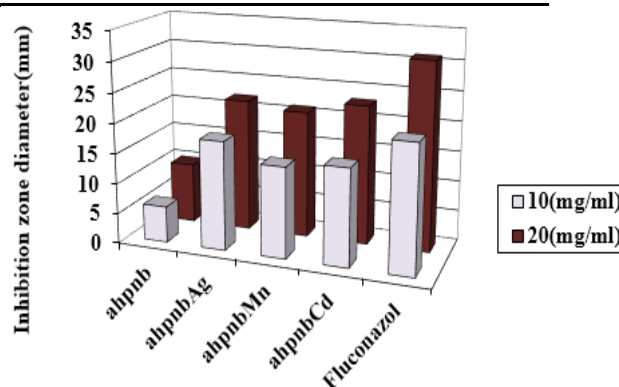
Table 5: Results of antibacterial activity of the prepared ligand and its complexes in DMSO.

Compounds	Inhibition zone (mm)					
	<i>Serratia marcescens</i> (-ve)		<i>Escherichia coli</i> (-ve)		<i>Micrococcus luteus</i> (+ve)	
Conc. (mg/ml)	10	20	10	20	10	20
ahpnb	6	10	5	8	11	14
ahpnbCd	13	23	11	16	18	32
ahpnbMn	13	22	10	16	18	31
ahpnbAg	16	26	13	19	23	36
Ofloxacin	22	31	17	24	27	41

pH-profile presented in (Figure.3) showed dissociation curves and a great stability pH range (4–10) of the prepared complexes. This means that the formation of the complex widely stabilizes the Schiff base. Consequently, the suitable pH range for the different applications of the prepared complexes is from pH = 4 to pH = 10 [2, 3, 9, 15]. The results of elemental analysis, molar conductance, magnetic susceptibility, infrared and electronic spectra help to know the suggested structure of the complexes.

3.9. Antimicrobial Activity

The *in vitro* antimicrobial activities of the synthesized Schiff base ligands and their corresponding metal complexes against three selected bacteria (*Escherichia coli*, *Micrococcus luteus* and *Serratia marcescens*) and three kinds of fungi (*Aspergillus flavus*, *Geotrichum candidum* and *Fusarium oxysporum*), were determined.

**Figure. 4:** Zone of inhibition against *Escherichia coli* (bacteria) by the prepared ligand and its prepared complexes.**Figure. 5:** Zone of inhibition against *Fusarium oxysporum* (fungi) by the prepared ligand and its prepared complexes.

Any chemotherapeutic agent diminishes the growth of microbes by microcidal or microstatic mechanisms. All of the tested compounds showed good biological potency against the micro-organism. On comparing the biological activities of the Schiff base ligands and their transition metal complexes with a standard bactericide and fungicide, it was shown that the metal complexes had moderate potency as matched with the standard but all the complexes were more active than their respective ligand. The higher inhibition zone of the transition metal complexes than those of the ligands can be explained based on the Overtone concept and the chelation hypothesis. Upon chelation, the polarity of the metal ion is reduced to a great extent due to the overlap of the ligand orbital and the fractional participating of the positive charge of the metal ion with donor groups. Furthermore, it expands the delocalization of the π -electrons over the whole chelating ring and enhances the permeation of the complexes into lipid membranes and the closing of the metal binding sites in the enzymes of micro-organisms [2, 3, 15, 31-34].

Table 6: Results of antifungal activity of the prepared ligand and its complexes in DMSO.

Compounds	Inhibition zone (mm)					
	<i>Aspergillus flavus</i>		<i>Getrichm candidum</i>		<i>Fusarium oxysporum</i>	
Conc. (mg/ml)	10	20	10	20	10	20
ahpnb	4	7	12	15	6	10
ahpnbCd	11	16	18	32	16	23
ahpnbMn	10	16	18	31	15	21
ahpnbAg	11	15	17	30	13	20
<i>Fluconazol</i>	15	24	24	39	21	31

Table 7: Spectral parameters for DNA interaction with the synthesized complexes.

Complex	λ_{max} Free (nm)	λ_{max} Bound (nm)	Δn (nm)	Chromism (%) ^a	Type of Chromism	Binding Constant $K_b \times 10^6 \text{ mol}^{-1} \text{ dm}^3$	ΔG^\ddagger KJ mol^{-1}
ahpnbCd	391	390	1	20.6	Hypo	0.05 ± 0.02	-26.79
	315	316	1	20.3	Hypo		
ahpnbMn	442	443	1	39.4	Hypo	0.11 ± 0.02	-28.89
	346	347	1	27.8	Hypo		
ahpnbAg	439	438	1	21.2	Hypo	0.04 ± 0.02	-26.47
	392	395	3	21.1	Hypo		

$$^a \text{Chromism (\%)} = [(\text{Abs}_{\text{free}} - \text{Abs}_{\text{bound}}) / \text{Abs}_{\text{free}}]$$

The results of the investigations explicate the antipathogenic behavior of the compounds and this efficacy is positively altered on complexation. data are listed in Table (5,6) and Figure (4,5).

3.10. DNA binding activity

3.10.1. Electronic spectra of interaction with DNA

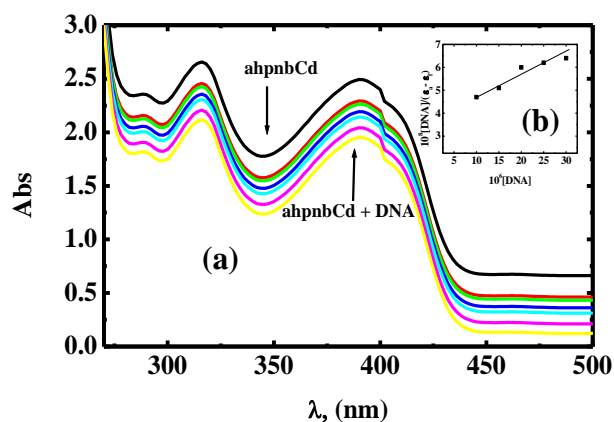


Figure. 6: (a) Spectral scans of the interaction of ahpnbCd complex (10 μM) in 0.01 M Tris buffer (pH= 7.5, 25°C) with CT DNA (from top to bottom, 0–40 μM DNA, at 5μM intervals). (b) Plot of $[\text{DNA}]/(\epsilon_a - \epsilon_f)$ vs. $[\text{DNA}]$ for the titration of DNA with ahpnbCd complex.

Titration with electronic absorption spectroscopy is an effective route to investigate the binding mode of DNA with metal complexes. The spectra were recorded as a function of the addition of the buffer solutions of

reprocessed CT-DNA to the buffer solutions of the metal complexes.

If the binding system is intercalation, the orbital of the intercalated ligand can conjugate with the orbital of the base pairs, reducing the $\pi - \pi^*$ transition energy and producing bathochromism. If the jointing orbital is partially filled by electrons, it results in deficiency the transition probabilities and producing hypochromism [2, 3, 15, 35]. The extent of the hypochromism or hyperchromism in the metal-to-ligand charge transfer (MLCT) band is usually consistent with the strength of intercalative interaction [2, 3, 15, 36]. The electronic absorption spectra of ahpnbCd complex in the absence and presence of different concentrations of buffered CT-DNA are given in (Figure.6). Addition of increasing amounts of CT-DNA resulted in a decrease of absorbance for a complex. The spectral parameters for the DNA interaction with the prepared complexes are shown in in (Table7). The investigated complexes could link to DNA via an intercalative mode with the sequence: ahpnbAg> ahpnbCd> ahpnbMn.

3.10.2. Viscosity measurements

For indicating the interaction nature between the prepared complexes and DNA, viscosity measurements were carried out. Hydrodynamic methods such as viscosity measurements which are sensitive to length increase or decrease of DNA are regarded as the most operative means of studying the binding mode of complexes to DNA in the absence of crystallographic structural data and NMR. For further clarification of the binding mode, viscosity measurements were carried out.

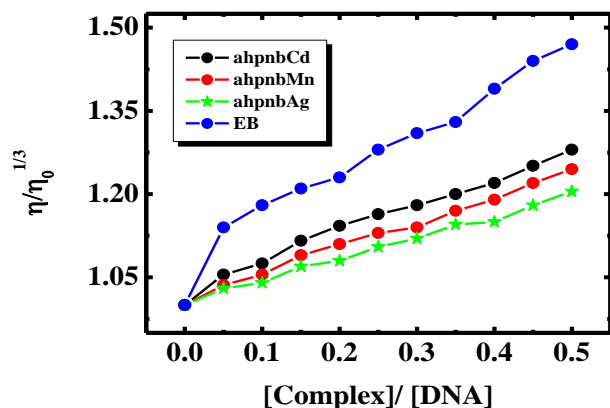


Figure. 7: The effect of increasing the amount of the synthesized complexes on the relative viscosities of DNA at [DNA] =250 μM, [complex] =10–250 μM and 298 K.

Under appropriate circumstances, a classical intercalative mode such as intercalation of drugs like ethidium bromide (EB) causes a remarkable increase in the viscosity of DNA solution due to an increase in the separation of base pairs at the intercalation site and hence an expand in the overall DNA length. On other hand, drug molecules binding exclusively to the DNA grooves cause less pronounced in DNA solution viscosity [37] a partial intercalation of complex may bend the DNA helix, producing the decrease of its operative length and, concomitantly, its viscosity [38]. The relative viscosity of DNA solution increases greatly as the amount of the complex increases, as shown in (Figure.7). This may be due to the accession of the aromatic ring in Schiff base ligand into the DNA base pairs resulting in a bend in the DNA helix, hence, expand in the separation of the base pairs at the intercalation site and increasing in DNA molecular length. Moreover, the sequence of the notified increase in the values of viscosity was correlated with the binding affinity to DNA i.e. ahpnbCd complex shows the highest binding affinity to DNA and the highest viscosity.

3.10.3. Gel electrophoresis

Agarose gel electrophoresis is utilized for the DNA cleavage studies. The Schiff base Cd(II), Mn(II) and Ag(I) complexes were studied for their DNA binding activity by agarose gel electrophoresis method (Figure.8).

The gel after electrophoresis obviously indicated that the intensity of all the treated DNA samples has partially diminished, possibly because of the cleavage of the DNA. The partial cleavage of DNA was observed in Cd(II), Mn(II) and Ag(I) complexes of the Schiff base. The difference was notified in the bands of the complexes compared to that of the control DNA. This clarifies that the control DNA alone does not show any patent cleavage whereas the complexes show cleavage [39]. However, the nature of reactive intermediates embraced in the DNA

cleavage by the complexes is not clear [40]. These results indicate that the metal ions play an important role in the cleavage of isolated DNA. As the compound was notified to cleave the DNA, it can be deduced that the compound inhibits the growth of the pathogenic organism by cleaving the genome. The studies reveal that partial cleavage of DNA was observed by Cd(II), Mn(II) and Ag(I) complexes. The experimental findings indicated that the investigated complexes could bind to DNA via intercalative mode.

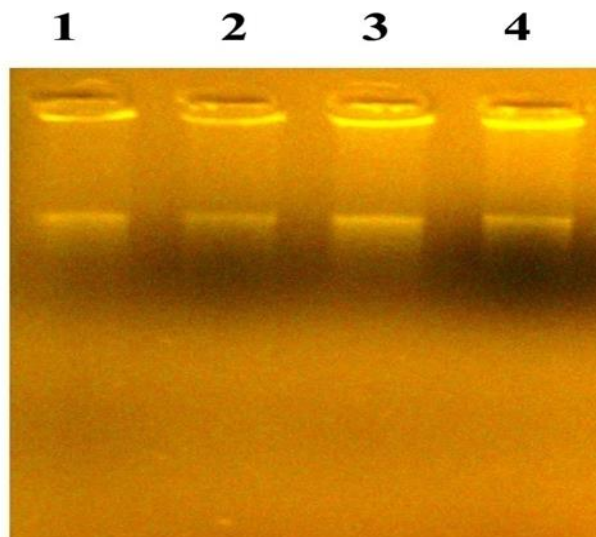


Figure. 8: DNA binding study Calf-thymus (CT) -DNA with Cd (II), Mn (II) and Ag (I) complexes. Lane1: Ag (I) ; Lane 2: Cd (II) ; Lane 3: Control DNA ; Lane 4: Mn (II).

4 Conclusion

Some new Schiff base complexes have been synthesized and characterized by different analytical tools. The analytical data showed the presence of one metal ion per two ligand molecule and suggested structure for the complexes $[M(L_1)_2(H_2O)_2].nH_2O$ except silver complex, its suggested structure is $[M(L_1)(H_2O)_2].H_2O$. The electronic spectral data is in favor of an octahedral geometry of the Complexes except silver complex, which is tetrahedral. The ligand and its Cd(II), Mn(II) and Ag(I) complexes were tested for antimicrobial activity against some pathogens. All the complexes were found to be more active against the bacteria and fungi, whereas the ligand showed the least antimicrobial activity against the bacteria and fungi. The DNA interaction of these compounds was tested by using gel electrophoresis and viscosity measurements. The experimental results showed that the investigated complexes could bind to DNA via intercalative mode.

References

- [1] Ahmed. M. Abu-Dief and Ibrahim M. A. Mohamed, Beni-Suef University Journal of Basic and Applied Sciences, 4, 2, 119–133 (2015).

- [2] L. H. Abdel Rahman, A. M. Abu-Dief, N. A. Hashem, A. A. Seleem, *Int. J. Nano. Chem.*, 1(2) 79 – 95(2015).
- [3] L. H. Abdel-Rahman, A. M. Abu-Dief, E. F. Newair, S. K. Hamdan, *J. Photochem. & Photobiol. B: Biology*, 160, 18–31(2016).
- [4] M. M. Abd-Elzaher, *Journal of the Chinese Chemical Society*, 48, 153–158, (2001).
- [5] A. A. Jarrahpour, M. Motamedifar, K. Pakshir, N. Hadi, and M. Zarei, *Molecules*, 9, 815–824, (2004).
- [6] Kou-San Ju and Rebecca E. Parales, *Microbiol Mol Biol Rev*, 74, 250–272, (2010).
- [7] Z. Hong, *Trans. Metal. Chem.*, 33, 797, (2008).
- [8] Prafullkumar A. Kulkarni, Seema I. Habib, Devdatta V. Saraf, Mrunalini M. Deshpande, *RJPBCS*, 3, 107, (2000).
- [9] L. H. Abdel-Rahman, R. M. El-Khatib, L. A. E. Nassr, A. M. Abu Dief, *Journal of Molecular Structure*, 1040, 9-18, (2013).
- [10] Disha Tilala, Hardik Gohe, Vishw Dhinoj, Denish Kari, *Int.J.ChemTech Res.* 5, 2330, (2013).
- [11] L. H. Abdel-Rahman, R. M. El-Khatib, L. A. E. Nassr, A. M. Abu-Dief, F. El-Din Lashin, *Spectrochimica Acta Part A: Molecular Biomolecular Spectroscopy*, 111, 266–276, (2013).
- [12] L. H. Abdel-Rahman, R. M. El-Khatib, L. A. E. Nassr, A. M. Abu-Dief, *International Journal of Chemical Kinetics* 46 (9), 543-553 (2014)
- [13] L. H. Abdel-Rahman, R. M. El-Khatib, L. A. E. Nassr, A. M. Abu-Dief, *Russian Journal of General Chemistry*, 84, 1830–1836, (2014).
- [14] D. Sabolova, M. Kozurkova, T. Plichta, Z. Ondrusova, D. Hudecova, M. Simkovic, H. Paulikova, A. Valent, *Int. J. Bio. Macromol.* 48, 319–325, (2011).
- [15] L. H. Abdel-Rahman, R. M. El-Khatib, L. A. E. Nassr, Ahmed M. Abu-Dief, M. Ismail, A. A. Seleem, *Spectrochimica Acta Part A: Molecular and Biomolecular Spectroscopy* 117, 366, (2014).
- [16] N. Raman et al, *J. Chem. Sci.*, 119, 303–310, (2007).
- [17] N. Raman, S. J. Raja, J. Joseph, J. D. Raja, *J. Chil. Chem. Soc.*, 52, 1138, (2007).
- [18] A. Ourari, K. Ouari, W. Moumeni, L. Sibous, *Trans. Met. Chem.*, 31, 169, (2006).
- [19] Hany M. Abd El-Lateef, Ahmed M. Abu-Dief, L.H. Abdel-Rahman, Eva Carolina Sañudo, Núria Aliaga-Alcalde, *Journal of Electroanalytical Chemistry* 743, 120–133 (2015).
- [20] M. M. Omar, G. G. Mohammed, *Spectrochim. Acta, A* 61, 929, (2005).
- [21] A. P. Mishra, R. K. Mishra, S. P. Shrivastava, *J. Serb. Chem. Soc.* 74, 523, (2009).
- [22] M. A. Neelakantan, S. S. Marriappan, J. Dharmaraja, T. Jeyakumar, K. Muthukumar, *Spectrochim. Acta, A* 71, 628, (2008).
- [23] Ahmed M. Abu-Dief, Raul Díaz-Torres, Eva Carolina Sañudo, Laila H. Abdel-Rahman, Núria Aliaga-Alcalde, *Polyhedron* 64, 203–208(2013).
- [24] F. Ahmad, M. Parvez, S. Ali, M. Mazhar, A. Munir, *Synth. React. Inorg. Met. Org. Chem.* 32, 665–687, (2002).
- [25] D. X. West and A. A. Nasar, *Trans. Met. Chem.* 24, 617–621, (1999).
- [26] Laila H. Abdel-Rahman, Ahmed M. Abu-Dief, Rafat M. El-Khatib, Shima M. Abdel-Fatah, *Journal of Photochemistry and Photobiology B: Biology*, 162, 298–308 (2016).
- [27] E. Canpolat and M. Kaya, *J. Coord. Chem.* 55, 961–968, (2002).
- [28] Jain and Mishra, *J. Serb. Chem. Soc.* 77, 1013–1029, (2012).
- [29] Laila H. Abdel-Rahman, Ahmed M. Abu-Dief, Samar Kamel Hamdan and Amin Abdou Seleem, *Int. J. Nano. Chem.* 1, 65-77 (2015).
- [30] H.M. Abd El-Lateef, A.M. Abu-Dief, B. E. M. El-Gendy, *J. Electroanal. Chem.*, 758, 135–147 (2015).
- [31] L. H. Abdel-Rahman, A. M. Abu-Dief, M., Ismael, M. A. A., Mohamed, N. A. Hashem, *J. Mol. Struct.*, 1103, 232 – 244 (2016)
- [32] Z. H. Chohan, H. Pervez, A. Rauf, K. M. Khan, C. T. Supuran, *J. Enzym. Inhib. Med. Chem.* 39, 417, (2004).
- [33] R. R. Coombs, S. A. Westcott, A. Decken, F. J. Baerlocher, *Transition Met. Chem.* 30, 411, (2005).
- [34] A. M. Abu-Dief and L. A. E. Nassr, *J. Iran. Chem. Soc.*, 12 943-955 (2015)
- [35] A. M. Pyle, J. P. Rehmman, R. Meshoyrer, C. V. Kumar, N. J. Turro, J. K. Barton, *J. Am. Chem. Soc.* 111, 3051–3058, (1989).
- [36] X. W. Liu, J. Li, H. Li, K. C. Zheng, H. Chao, L. N. Ji, *J. Inorg. Biochem.* 99, 2372–2380, (2005).
- [37] S. Shi, J. Liu, J. Li, K. C. Zheng, X. M. Huang, C. P. Tan, L. M. Chen, L. N. Ji, *J. Inorg. Biochem.* 100, 385–395, (2006).
- [38] Y. Liu, W. Mei, J. Lu, H. Zhao, L. He, F. Wu, *J. Coord. Chem.* 61, 3213–3224, (2008).
- [39] An and Prakash Mishra, Herhita purwar Rajendra kumar jain *Biointerface research*, 2, 291-299, (2012).
- [40] G. Yang, F. Z. Wu, L. Wang, L. Nian Fi and X. Tina, *J. Inorg Biochem.*, 66, 141-144, (1997).